

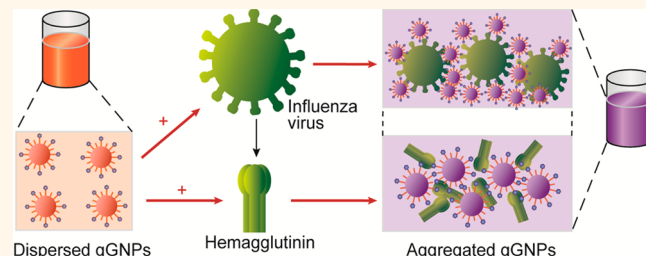
Analysis of Influenza Virus Receptor Specificity Using Glycan-Functionalized Gold Nanoparticles

Jinhua Wei,^{†,‡,§,⊥} Longtang Zheng,^{†,‡,⊥} Xun Lv,^{†,⊥} Yuhai Bi,[†] Wenwen Chen,[§] Wei Zhang,[†] Yi Shi,[†] Lei Zhao,[†] Xiaoman Sun,^{†,‡} Fei Wang,^{†,‡} Shuihong Cheng,[†] Jinghua Yan,[†] Wenjun Liu,[†] Xingyu Jiang,[§] George F. Gao,[†] and Xuebing Li^{†,*}

[†]CAS Key Laboratory of Pathogenic Microbiology and Immunology, Institute of Microbiology, Chinese Academy of Sciences, Chaoyang District, Beijing 100101, China,

[‡]Graduate University of Chinese Academy of Sciences, Shijingshan District, Beijing 100049, China, and [§]CAS Key Laboratory for Biological Effects of Nanomaterials and Nanosafety, National Center for NanoScience and Technology, Zhongguancun, Beijing 100190, China. [⊥]These authors contributed equally.

ABSTRACT Recent cases of human infection with avian influenza H5N1 and H7N9 viruses underscore an urgent need for techniques that can rapidly assess their potential threat to the humans. Determination of the receptor-binding property of influenza virus is crucial to direct viral control and prevention measures. Current methods to perform this analysis are dependent on immunoanalytical strategies that use unstable biological components and complex procedures. We have developed a facile colorimetric assay to determine the interaction of the viral hemagglutinin (HA) protein with host glycan receptors using glycan-functionalized gold nanoparticles (gGNPs). This method is based on the color and absorbance changes of gold probes when the solution is simply mixed with HAs or intact viruses. The resulting sensitivity and selectivity has enabled HA/virus binding to various glycan structures to be differentiated visually and rapidly. Using this system, we have screened, in parallel, the receptor specificity of eight representative human and avian viral HAs and three whole viruses including an emerging H7N9 strain. Our results reveal the detailed receptor-binding profiles of H7N9 virus and its HA and show that they effectively bind to human-type receptors. This gGPNP-based assay represents a strategy that would be helpful for developing simple and sensitive systems to probe glycan-mediated biological processes.



KEYWORDS: glycan · gold nanoparticle · influenza virus · receptor specificity · sialic acid

Binding of influenza virus to host receptors is an essential step for its infection and transmission. This process is mediated by the specific interaction of a viral envelope protein, hemagglutinin (HA), with the host surface glycan receptors containing terminal sialic acid (SA). In general, avian-adapted viruses prefer the α 2,3-linked SA receptors that are commonly found on the intestinal epithelia of birds. Human-adapted viruses preferentially bind to receptors with an α 2,6 configurations that are predominately expressed in the upper respiratory tract of humans.¹ All known subtypes of the influenza A virus and all serotypes of HA (H1–H16) can be found in wild birds, with the exception of the H17N10 subtype recently found in bats.² Therefore, avian species are thought to be the natural reservoirs of the influenza A virus.

With respect to adaptation of avian viruses to the human population, a shift in HA-binding preferences to human receptors, either through genetic reassortment or mutations, is necessary. Evidence suggests that previous pandemic viruses, H1N1 in 1918 and 2009, H2N2 in 1957, and H3N2 in 1968, were of avian origin but acquired a preference for human receptors.^{3–6} Several other avian subtypes, such as the highly pathogenic avian H5N1 virus, continue to cause localized outbreaks in domestic poultry worldwide. In certain cases, they can infect humans directly without changing their inherent avian receptor preference.⁷ The emerging avian H7N9 virus in China possesses the ability to infect humans,⁸ fuelling concerns that H7N9 and H5N1 could evolve into pandemic strains.

Analyzing the receptor specificity of influenza viruses is crucial in assessing their

* Address correspondence to lixb@im.ac.cn.

Received for review January 15, 2014 and accepted April 13, 2014.

Published online April 14, 2014
10.1021/nn5002485

© 2014 American Chemical Society

potential threat to the public. Several methods are currently available to conduct these analyses; these include glycan⁹ and neoglycolipid¹⁰ microarray assays, solid-phase binding assays,¹¹ enzyme-linked immunosorbent assays (ELISAs),¹² and hemadsorption assays.¹³ The analyses based on these methods have improved our knowledge regarding the complexity and diversity of influenza virus binding. However, there are some limitations to these assays, such as their labor-intensive nature and the instability of specific biological components, thereby restricting their use to specialized laboratories. Recently, technologies involving surface plasmon resonance (SPR) of gold sensor chips,^{14,15} microscale thermophoresis,¹⁶ and surface biolayer interferometry¹⁶ have been tested; however, these methods rely on advanced instruments and are low throughput.

Our assay exploits the distance-dependent optical properties of gold nanoparticles (GNPs).¹⁷ Coupled with multiple copies of SA receptors on their surface, the GNPs allow virus/HA binding to be detected visually and using spectroscopy (Figure 1). Monodispersed glycan-functionalized GNPs (gGNPs) absorb a narrow band of light (maximum absorbance 522 nm) because of the SPR of gold probes, making the solution appear red. Subsequent binding with trimeric HAs or viruses results in gGPNP aggregates, leading to a red shift in SPR absorbance and thus a visible color change of the solution to purple. Because the size and extent of aggregates are dependent on binding ability, distinct signal response patterns indicate binding specificity and affinity. The use of GNPs for colorimetric sensing was pioneered in 1980¹⁸ and has since been developed for the detection of nucleic acids, proteins, carbohydrates, and metal ions.^{19–23} The detection of influenza virus using this strategy was also reported recently.^{24–26} A key advantage of using gGPNP probes is that glycan multivalency can confer an avidity effect, which is known to increase generally weak individual protein–glycan interactions.²⁷ Here, we present the design and construction of gGNPs. We also demonstrate the use of these gGNPs to develop a simple method for the rapid detection of influenza virus receptor specificity.

RESULTS AND DISCUSSION

We developed two types of gGNPs, with either α 2,3 or α 2,6 linkages, that featured several typical structures of SA receptors⁹ (Figure 1A). These SA receptors, which are modified by *N*-acetylation, sulfation, and fucosylation, represent natural glycan sequences commonly found in cell surface glycoproteins and glycolipids.²⁸ We took into account three essential parameters that might affect binding capacity and assay sensitivity when designing the gGNPs. First, the high molar extinction coefficient of GNPs with a diameter of 13 nm ($2.7 \times 10^8 \text{ M}^{-1} \text{ cm}^{-1}$) allows them to appear red, even at nanomolar concentrations.²⁹ This enables sensitive detection of HA molecules or viruses, even at

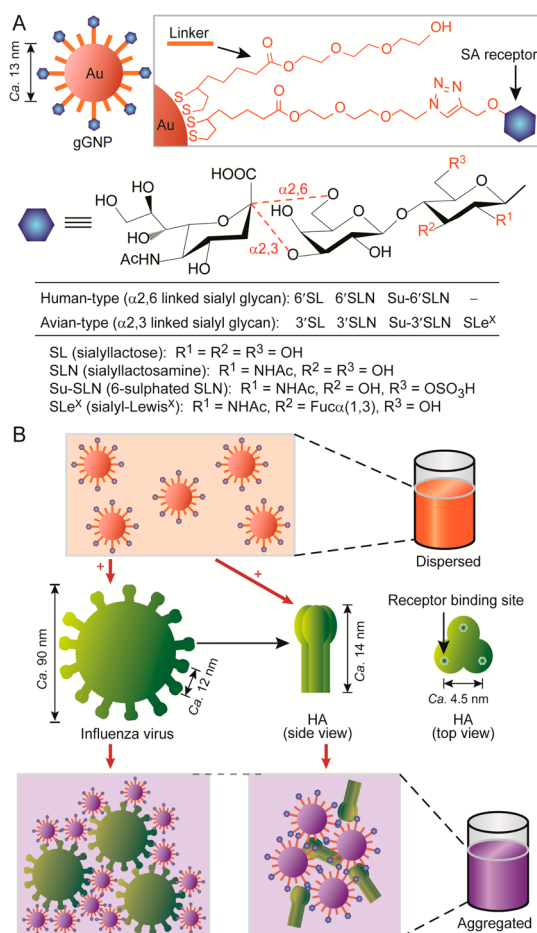


Figure 1. Structure of gGNPs (A) and mechanism of gGPNP-based assays (B). (A) In addition to SA receptors, a lactosamine (LN)-displaying gGPNP was also similarly synthesized (see Figure 2). (B) gGPNP aggregation was caused by its binding to HA or whole virus. This results in a visual red-to-purple shift. Concomitant changes in the SPR absorbance of gGNPs were measured by UV-vis spectroscopy to quantify binding specificity.

low concentration. The size of these nanoparticles is similar to that for HA and about an order of magnitude smaller than influenza viruses, allowing for easy formation of gGPNP–HA aggregates and attachment of multiple gGNPs to the virus surface, thus inducing a red shift in SPR absorbance. Second, the disulfide linker, consisting of an alkyl chain terminated with ethylene glycol groups, allows for the formation of self-assembled monolayers that can attach to the surface of GNPs.³⁰ This results in resistance to nonspecific adsorption, stable dispersion in aqueous media, and uniform orientation of SA receptors. Third, the SA receptors serve as selective recognition elements, with their hydrophilic features facilitating the solubility and stability of gGNPs.

Using the above-mentioned design elements, we developed a modular synthetic strategy that allowed for flexible synthesis of SA receptors and gGNPs (Figure 2 and Supporting Information Figure S1). The SA receptors (**10a–10g**), with a disulfide-terminated linker at the anomeric center, were

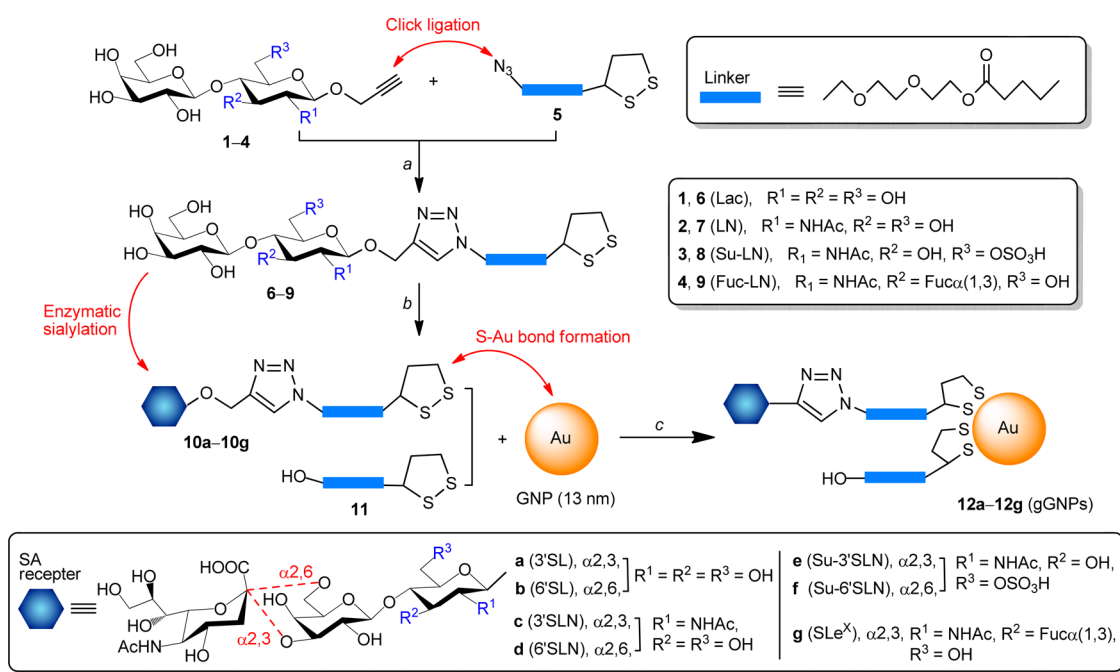


Figure 2. Chemoenzymatic synthesis of gGNPs. Reagents and conditions: (a) CuI , DMF/MeOH, rt, 50–80%; (b) $\alpha2,3\text{-SiaT}$ or $\alpha2,6\text{-SiaT}$, CMP-Neu5Ac, Tris-HCl buffer (pH 8.0), 37 °C, 2 h, 17–87%; (c) deionized water, rt, 24 h. Abbreviations: DMF, *N,N*-dimethylmethyformamide; rt, room temperature; SiaT, sialyltransferase; CMP, cytidine 5'-monophosphate; GNP, citrate-coated gold nanoparticle.

synthesized by “click” reactions of alkynes **1–4** with azide **5**, followed by enzymatic $\alpha2,3$ or $\alpha2,6$ sialylations. The disulfides enabled straightforward modifications of citrate-stabilized GNPs with SA receptors through ligand-exchange reactions,²⁹ yielding the desired gGNPs (**12a–12g**). This modular synthesis allows for easy expansion of the scope of gGNPs by incorporating a number of new glycans that would facilitate more comprehensive studies on influenza virus receptor specificity and other glycan-mediated biological processes by gGNPs.

All resulting gGNPs were fully characterized (Figure S2). Transmission electron microscopy (TEM) analysis revealed that modification of GNPs with glycans did not significantly affect their morphology. Ultraviolet–visible (UV–vis) spectroscopy measurement indicated no remarkable change between the absorbance of GNPs and gGNPs. Dynamic light scattering (DLS) assay demonstrated the slightly increased diameter of gGNPs compared to GNPs. MALDI-TOF MS analysis identified the incorporated glycans in gGNPs. In particular, through X-ray photoelectron spectroscopy and thermogravimetric analyses, all gGNPs were determined to have approximately 1600 glycan molecules per particle with a molar ratio of 4:1 to free linkers (glycan display level could be adjusted experimentally). The details of glycan number calculation are provided in the Supporting Information. As such, gGNPs with desirable structures and properties were systematically verified.

We cloned two recombinant HA proteins: an avian H5 from H5N1 A/Vietnam/1203/2004 (vieH5) with $\alpha2,3$

specificity, and a human H1 from H1N1 A/California/04/2009 (09H1) with $\alpha2,6$ specificity. These soluble proteins were expressed using a baculovirus system.^{14,15} We chose these HAs because their receptor-binding properties had been well-characterized.^{4,7,14} The HAs were mixed with gGNPs in phosphate-buffered saline (PBS) at room temperature. Combinations of 09H1 with 6'SLN–gGPNP and vieH5 with 3'SLN–gGPNP showed red shifts in SPR absorbance (Figure 3B,D) and concomitant red-to-purple changes (Figure 3I). These spectroscopic and color shifts could be attributed to the HA-induced formation of gGPNP aggregates (Figure 3F,H). In contrast, little or no changes were detected for other mixtures (Figure 3A,C and Figure S3), demonstrating the selectivity of this system. The specific HA–gGPNP interaction can also be verified by DLS experiments (Figure S4). Further analysis revealed that binding of HA with gGNPs to form aggregates was dependent on interaction time (Figure 3J). Changes in absorbance indicated that all interactions were completed within 80 min, with specific maximum A_{680}/A_{522} ratios that could be used to quantify relative binding affinities (Figure 3K). The color transitions, which were observed at 80 min after combining HAs with gGNPs, allowed easy differentiation of HA receptor specificity by the naked eye. The HA–gGPNP binding kinetics were also observed to be HA-concentration-dependent, with HAs at concentrations higher than 4.2 $\mu\text{g/mL}$, sufficient for producing visual and spectroscopic results (Figure S5). This sensitivity was comparable to that obtained from more traditional methods such as glycan microarrays and ELISAs.^{4,9,12}

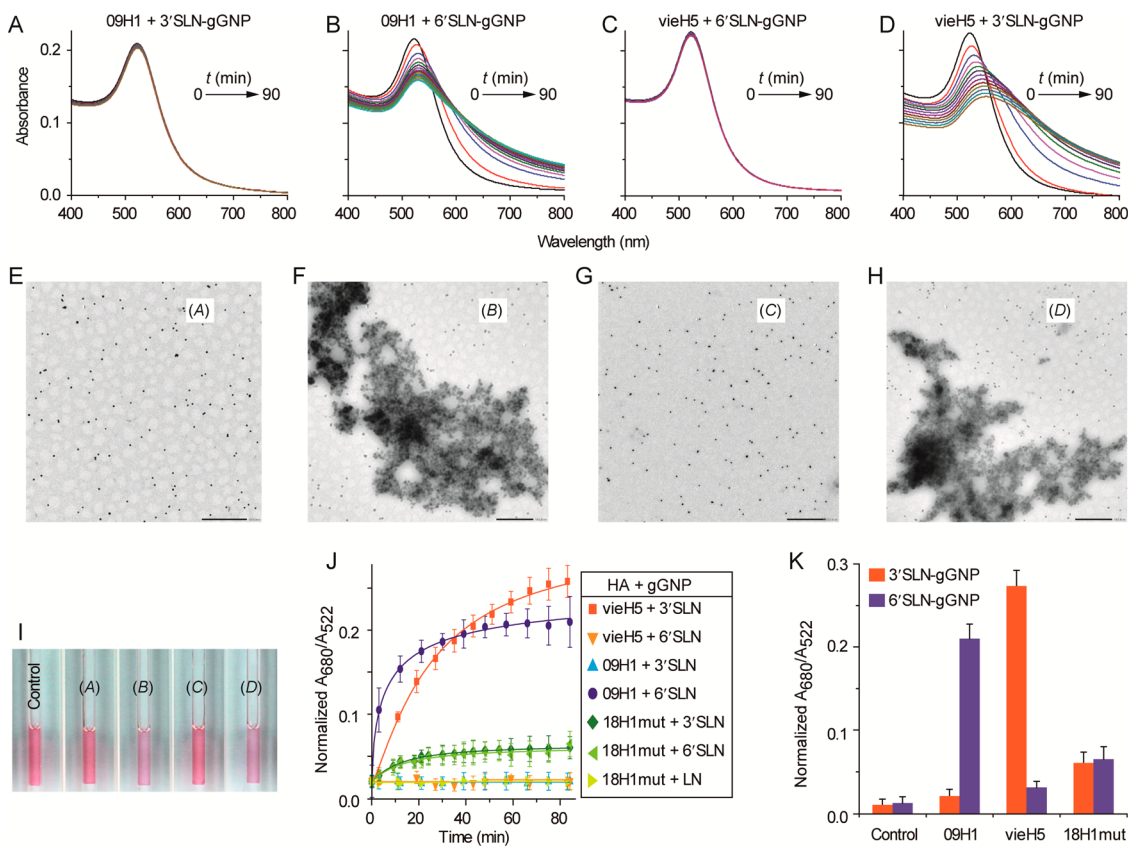


Figure 3. Analysis of HA binding to gGNPs. (A–D) UV–vis spectra of HA–gNP mixtures showing selective binding of 09H1 with 6'SLN–gGNP and vieH5 with 3'SLN–gGNP. (E–H) TEM images of HA–gNP interactions corresponding to A–D. These show 6'SLN–gGNPs aggregated with 09H1 (F) and 3'SLN–gGNPs aggregated with vieH5 (H). Scale bars indicate 500 nm. (I) HA–gNP mixtures corresponding to A–D, showing red-to-purple shifts. (J) Kinetics of HA–gNP interactions. Normalized A_{680}/A_{522} values at 80 min were used for assessing the relative binding affinity of HAs. The 18H1mut is a D225G mutant (H3 numbering) of 18H1 HA from a pandemic H1N1 virus (A/South Carolina/1/18). This mutant has mixed α 2,3/ α 2,6 specificity.^{9,14} Error bars indicate standard deviations from three independent experiments. (K) Relative binding affinity of HAs to gGNPs. Error bars indicate standard deviations from three independent experiments.

Collectively, these experiments demonstrate a simple, fast, selective, and sensitive strategy for determining HA–glycan interactions.

We applied this method to investigate the receptor specificity of a H7 HA, designated anhH7, which was generated from an emerging human-infecting H7N9 A/Anhui/1/2013 virus.⁸ Characterizations of this virus, including the global receptor preference, have recently been conducted.^{8,31–33} Using X-ray crystallography, our group and others have previously showed that anhH7 bound to both α 2,3 and α 2,6 SLNs;^{15,34} however, details of the anhH7 bindings to other SA receptors remain unclear. To validate our results, we also included several typical avian and human virus HAs as controls to enable direct comparison with previously reported results (Figure 4). Using predetermined conditions, we conducted the assays in a high-throughput manner. Interactions of eight HAs in combination with seven gGNPs were screened in parallel. HAs from human-adapted viruses (09H1, 18H1, 68H3) prefer α 2,6 gGNPs (Figure 4A), whereas those from avian-adapted viruses (vieH5, qinH5, sheH5) favor α 2,3 gGNPs (Figure 4B). The 18H1mut exhibits relatively weak

and mixed α 2,6/ α 2,3 specificity. These binding patterns are distinct for each HA and are largely consistent with those from previous studies,^{4,7,9,13,14,34,35} confirming the ability and reliability of our system. Similar to glycan microarray analysis,⁹ this method permits discrimination of HA-binding preference for not only SA linkages but also fine modifications in SA receptors such as *N*-acetylation, sulfation, and fucosylation. For anhH7, our assay reveals a dual human/avian receptor preference. This is significant when compared with other HAs tested in this study, suggesting the possibility of anhH7 as an intermediate in avian H7 HA evolution that would eventually facilitate H7N9 virus adaptation to humans. Additionally, the observed α 2,6 specificity of anhH7 supports a recent study demonstrating that this HA can weakly attach to human respiratory tissues.³⁶

Analysis of HA proteins provides a basis for further studies on the H7N9 virus. We rescued the A/Anhui/1/2013 strain using reverse genetics technology¹⁵ to enable the virus-binding study. The rescued virus was designated anhH7N9. The gGNP-based assay was adjusted for screening whole viruses using a laboratory standard H1N1 strain, A/Puerto Rico/8/34 (PR8), which

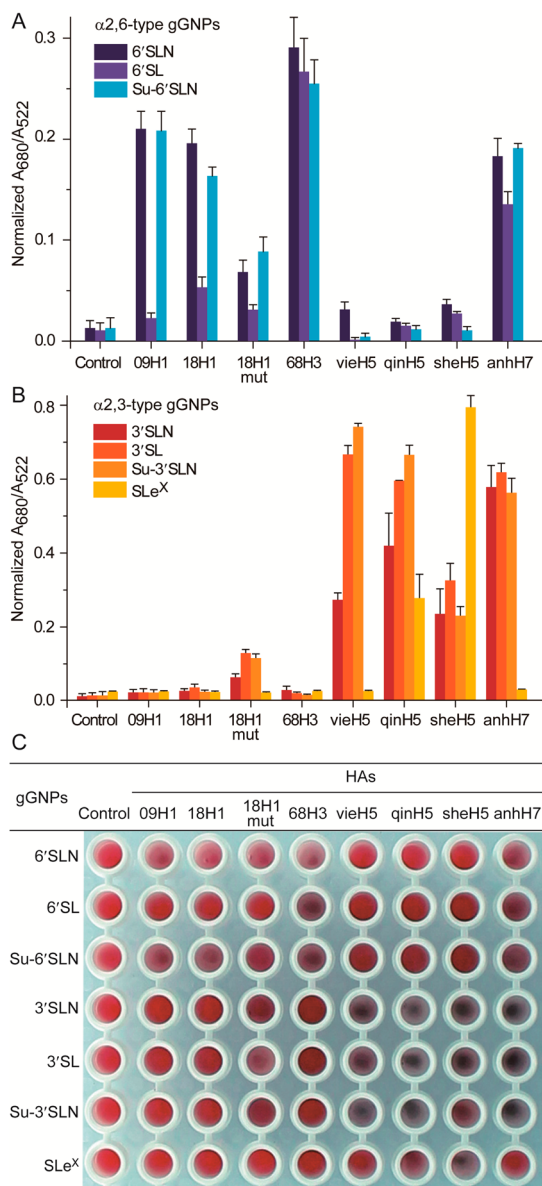


Figure 4. Analysis of the receptor specificity of H7N9 HA compared to several representative human and avian viral HAs. The 68H3 HA was generated from a pandemic H3N2 A/ Aichi/2/1968 strain. The qinH5 and sheH5 HAs were from two avian H5N1 viruses, A/Bar-headed Goose/Qinghai/1/2005 and A/Shenzhen/1/2011, respectively. (A) HAs binding to α 2,6-type gGNPs. Error bars reflect standard deviations from three independent experiments. (B) HAs binding to α 2,3-type gGNPs. Error bars reflect standard deviations from three independent experiments. Note that the scale of panel A is different from B because of the relatively low affinity of HAs to α 2,6-type gGNPs. (C) Colorimetric results of HA-binding assays.

has known binding specificity for α 2,3 glycans³⁷ (Figure 5 and Figure S6A–C). We used HA titer to represent the virus concentrations. This unit was determined by hemagglutination assay, which employs the viral binding to animal red blood cells to cause the aggregation for visual analysis.^{11,12,38} The kinetics of virus binding with gGNPs is faster than that for HAs, with virus–gGNP interaction complete within 30 min (Figure S6D). Only a small amount of virus (10 HA titer)

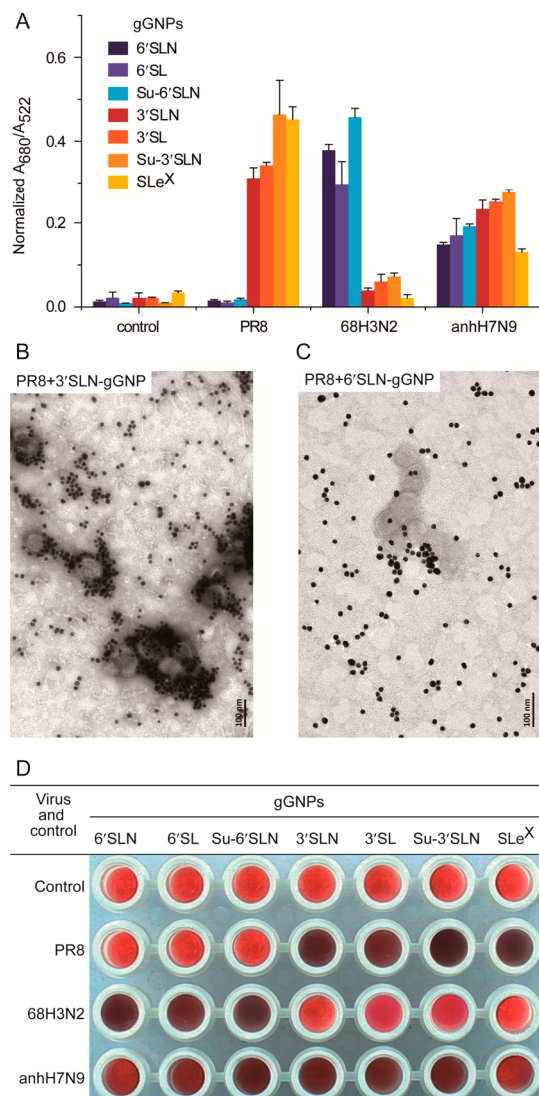


Figure 5. Analysis of H7N9 virus receptor specificity compared with the PR8 and 68H3N2 viruses. (A) PR8 and 68H3N2 viruses specifically bound to α 2,3- and α 2,6-type gGNPs, respectively, while anhH7N9 virus bound to both types of gGNPs. (B) TEM analysis showing 3'SLN–gGNP aggregates due to PR8 virus binding. Scale bars indicate 100 nm. (C) Dispersed 6'SLN–gGNPs in the presence of PR8 virus. Scale bars indicate 100 nm. (D) Colorimetric results of virus-binding assays.

could result in marked spectral change (Figure S6E) and a rapid color shift (Figure 5D). These results indicate that increased HA valency on the viral envelope, in addition to multiple copies of SA receptors on the gGNP surface, confers a high avidity interaction that leads to fast and sensitive detection of virus binding. We also analyzed a human-adapted H3N2 virus, A/Aichi/1/1968 (68H3N2), which clearly shows α 2,6 specificity.^{6,13} The assay of anhH7N9 virus revealed that it bound to both α 2,3 and α 2,6 receptors, in accordance with the results obtained for anhH7 HA. The ability of anhH7N9 virus to effectively bind to human receptors correlates with results from recent studies showing its efficient replication in cells derived from the respiratory tract of humans and other mammals.^{8,31,32}

An important aspect in the prevention and control of influenza is continuous monitoring of the evolution of all circulating strains in humans and animals to gauge the potential for pandemics and to direct vaccine/drug designs. In general, the study of receptor-binding properties of a particular influenza virus, or its HA, necessitates the analysis of a number of relevant strains/HAs for comparison. Colorimetric detection would be convenient because it is simple and easily applicable to high-throughput systems. The ability of gGNP-based assays for quickly screening the specificity of HAs and viruses was shown in our study (Figure 4C and Figure 5D). These results can be visually discriminated, providing a technique for simultaneously screening receptor specificity of a range of HA proteins or viruses.

CONCLUSIONS

We report a gGNP-based assay method for the determination of influenza virus receptor specificity.

This method is conceptually different from conventional techniques currently in use. Unlike plate- and chip-based assays in which the analyte must be immobilized to a solid surface, free gGNPs and viruses/HAs in medium are able to partake in a dynamic binding process that allows the avidity effect to be fully exploited. The results from our system rely on the unique optical properties of GNPs, as opposed to fluorophore- and/or enzyme-conjugated antibodies. This results in our assays being easier to conduct and enables immediate analysis of emerging viruses without the need of an antibody against that virus. Finally, visual detection without the aid of any instruments makes this method ideal for developing a portable device that can be used in the field. This gGNP-based assay represents a strategy that would be helpful for developing simple and effective techniques to probe glycan-mediated biological processes, which is ubiquitous in living systems.

MATERIALS AND METHODS

Synthesis of gGNPs. Citrate-coated GNPs (13 nm in diameter) were prepared by the reduction of HAuCl_4 .³⁹ Using ligand-exchange reactions,²⁹ gGNPs were generated from these GNPs by treatments with disulfide-modified SA receptors **10a–10g** and free linker **11** (Figure 2). Briefly, **10a–10g** in deionized water (10 mM, 62.5 μL) and **11** in methanol (50 mM, 2.5 μL) were added to a solution of GNPs in deionized water (1.4 nM, 10.5 mL). The mixtures were stirred at rt for 24 h followed by centrifugation at 14 000 rpm for 30 min. The resulting gGNPs were separated, washed with deionized water, and redispersed in PBS (pH 7.4). Concentrations of GNPs and gGNPs in media were determined using UV-vis spectroscopy.⁴⁰ Synthesis and characterization of **10a–10g**, **11**, and other intermediate compounds are detailed in the Supporting Information.

Cloning, Expression, and Purification of HA. The cloning, expression, and purification of HA proteins were performed as previously described.¹⁴ The genes encoding the ectodomains of HAs from A/California/04/2009 (H1N1), A/South Carolina/1/18 (H1N1), A/Aichi/2/1968 (H3N2), A/Bar-headed Goose/Qinghai/1/2005 (H5N1), A/Shenzhen/1/2011 (H5N1), A/Vietnam/1203/2004 (H5N1), and A/Anhui/1/2013 (H7N9) were cloned into baculovirus transfer vector pFastBac1 (Invitrogen). The constructs also contain an N-terminal gp67 signal peptide for secretion, a C-terminal thrombin cleavage site, a trimerization foldon sequence, and a His6-tag at the extreme C-terminus. The 18H1-D225G mutants (18H1mut) were constructed by site-directed mutagenesis. Transfection and virus amplification were carried out according to the Bac-to-Bac baculovirus expression system manual (Invitrogen). HA proteins were produced by infecting suspension cultures of Hi5 cells (Invitrogen) for 2 days. Soluble HA was recovered from the cell supernatant by metal affinity chromatography using a 5 mL HisTrap HP column (GE Healthcare), then purified by ion-exchange chromatography (IEX) using a Mono-Q 4.6/100 PE column (GE Healthcare). The HA fractions were further purified using a membrane concentrator (Millipore) with a molecular weight cutoff of 10 kDa.

Preparation of Virus. A/Puerto Rico/8/34 (H1N1) was a stock in our laboratory. A/Anhui/1/2013 (H7N9) was generated using a reverse genetics method as previously described.¹⁵ Briefly, the eight genes of the H7N9 virus were synthesized and cloned into plasmid pHW2000. Cocultured MDCK and 293T cells (1:5) were transfected with eight plasmids (0.5 μg each). To the culture medium was added 0.9 mL of Opti-MEM (Invitrogen) containing

10 μL of lipofectamine 2000 (Invitrogen). After incubation at 37 °C for 6 h, the transfection mixture was removed from the cells and 1 mL of Opti-MEM containing 2 $\mu\text{g}/\text{mL}$ of TPCK-trypsin (Worthington Biochemical Corporation) was added. After 48 h of incubation, the supernatant was inoculated in specific pathogen-free chicken eggs to produce stock virus. A/Aichi/1/1968 was prepared from the genes of a pandemic H3N2 strain using a similar procedure. The rescued H7N9 and H3N2 viruses were sequenced to exclude any unwanted mutations and inactivated by treatment with 0.1% β -propiolactone before being used in gGNP-based assays. Virus concentrations were determined by hemagglutination assays with 1% chicken red blood cells. The virus generation and inactivation experiments were performed in approved biosafety level (BSL-3) containment laboratories.

gGNP-Based Assay. Solutions of HA (1 mg/mL) and gGPNP (2.8 nM) in PBS (pH 7.4) were prepared. Then, HA solution (2 μL) was mixed with gGPNP solution (120 μL) in a 200 μL quartz cuvette or in the well of a 96-well polystyrene microplate (Corning). The absorbance of mixtures was monitored at different time intervals using a UV-vis spectrophotometer (Hitachi U-2910) or a multimode reader (Infinite 200 PRO, Tecan). Normalized A_{680}/A_{522} values at 80 min were used to assess the relative binding affinity of HAs. The color of mixtures was observed in 8-strip PCR tubes (Genview). In HA-concentration-dependent binding assays, solutions of HA at different concentrations (0.0625–4 mg/mL) were used. In virus-binding assays, 12 μL of virus suspensions (256 HA titer) in the allantoic fluid of embryonated chicken eggs containing oseltamivir carboxylate (20 μM , Roche) was mixed with 88 μL of gGPNP solutions (2.5 nM, in PBS). The spectroscopic and colorimetric analyses were carried out according to the procedure described for HA-binding assays. Normalized A_{680}/A_{522} values at 30 min were used to assess the relative binding affinity of viruses. Viruses with varying concentrations (4–512 HA titer) were used for determining the concentration dependence of virus bindings.

TEM Analysis. Solutions containing gGPNP and HA were prepared as described for gGNP-based assays. After incubating these solutions for 80 min, aliquots (10 μL) were transferred with a pipet to carbon-coated copper TEM grids. The grids were left to stand at rt for 10 min. Then, excess liquid was removed with tissue paper, and the grids were air-dried before analysis. Similarly, samples for virus-binding analysis were prepared from suspensions containing virus and gGPNP (after 30 min of incubation). The grids were negatively stained using a 1%

aqueous solution of uranyl acetate (30 μ L) and air-dried before analysis. All samples were examined with a JEOL 1400 microscope operating at 100 kV.

DLS Analysis. Solutions containing gGNP and HA in quartz cuvettes were prepared according to the procedure described for gGNP-based assays. After 80 min of incubation, the cuvettes were applied to DLS measurement. Experiments were performed on a Zetasizer 3000HS instrument (Malvern) with a helium–neon laser source (632.8 nm) operating at a scattering angle of 90° and a temperature of 25 °C.

Conflict of Interest: The authors declare no competing financial interest.

Acknowledgment. We thank S. Sun and J. Ren for technical assistance. This work was financially supported by the Ministry of Science and Technology, China (973 Program, 2012CB518803), and the National Natural Science Foundation, China (Grant No. 81273381).

Supporting Information Available: Figures S1–S6; experimental procedures for the syntheses of SA receptors; characterization data of all new compounds; NMR and MS spectra. This material is available free of charge via the Internet at <http://pubs.acs.org>.

REFERENCES AND NOTES

1. Imai, M.; Kawaoka, Y. The Role of Receptor Binding Specificity in Interspecies Transmission of Influenza Viruses. *Curr. Opin. Virol.* **2012**, *2*, 160–167.
2. Tong, S.; Li, Y.; Rivailler, P.; Conrardy, C.; Castillo, D. A. A.; Chen, L.-M.; Recuenco, S.; Ellison, J. A.; Davis, C. T.; York, I. A.; et al. A Distinct Lineage of Influenza A Virus from Bats. *Proc. Natl. Acad. Sci. U.S.A.* **2012**, *109*, 4269–4274.
3. Gamblin, S. J.; Haire, L. F.; Russell, R. J.; Stevens, D. J.; Xiao, B.; Ha, Y.; Vasilth, N.; Steinhauer, D. A.; Daniels, R. S.; Elliot, A.; et al. The Structure and Receptor Binding Properties of the 1918 Influenza Hemagglutinin. *Science* **2004**, *303*, 1838–1842.
4. Xu, R.; McBride, R.; Nycholat, C. M.; Paulson, J. C.; Wilson, I. A. Structural Characterization of the Hemagglutinin Receptor Specificity from the 2009 H1N1 Influenza Pandemic. *J. Virol.* **2012**, *86*, 982–990.
5. Xu, R.; McBride, R.; Paulson, J. C.; Basler, C. F.; Wilson, I. A. Structure, Receptor Binding, and Antigenicity of Influenza Virus Hemagglutinins from the 1957 H2N2 Pandemic. *J. Virol.* **2010**, *84*, 1715–1721.
6. Lin, Y. P.; Xiong, X.; Wharton, S. A.; Martin, S. R.; Coombs, P. J.; Vachieri, S. G.; Christodoulou, E.; Walker, P. A.; Liu, J.; Skehel, J. J.; et al. Evolution of the Receptor Binding Properties of the Influenza A (H3N2) Hemagglutinin. *Proc. Natl. Acad. Sci. U.S.A.* **2012**, *109*, 21474–21479.
7. Stevens, J.; Blixt, O.; Tumpey, T. M.; Taubenberger, J. K.; Paulson, J. C.; Wilson, I. A. Structure and Receptor Specificity of the Hemagglutinin from an H5N1 Influenza Virus. *Science* **2006**, *312*, 404–410.
8. Zhou, J.; Wang, D.; Gao, R.; Zhao, B.; Song, J.; Qi, X.; Zhang, Y.; Shi, Y.; Yang, L.; Zhu, W.; et al. Biological Features of Novel Avian Influenza A (H7N9) Virus. *Nature* **2013**, *499*, 500–503.
9. Stevens, J.; Blixt, O.; Glaser, L.; Taubenberger, J. K.; Palese, P.; Paulson, J. C.; Wilson, I. A. Glycan Microarray Analysis of the Hemagglutinins from Modern and Pandemic Influenza Viruses Reveals Different Receptor Specificities. *J. Mol. Biol.* **2006**, *355*, 1143–1155.
10. Childs, R. A.; Palma, A. S.; Wharton, S.; Matrosovich, T.; Liu, Y.; Chai, W.; Campanero-Rhodes, M. A.; Zhang, Y.; Eickmann, M.; Kiso, M.; et al. Receptor-Binding Specificity of Pandemic Influenza A (H1N1) 2009 Virus Determined by Carbohydrate Microarray. *Nat. Biotechnol.* **2009**, *27*, 797–799.
11. Gambaryan, A. S.; Matrosovich, M. N. A Solid-Phase Enzyme-Linked Assay for Influenza Virus Receptor Binding Activity. *J. Virol. Methods* **1992**, *39*, 111–123.
12. Chandrasekaran, A.; Srinivasan, A.; Raman, R.; Viswanathan, K.; Raguram, S.; Tumpey, T. M.; Sasisekharan, V.; Sasisekharan, R. Glycan Topology Determines Human Adaptation of Avian H5N1 Virus Hemagglutinin. *Nat. Biotechnol.* **2008**, *26*, 107–113.
13. Rogers, G. N.; Paulson, J. C. Receptor Determinants of Human and Animal Influenza Virus Isolates: Differences in Receptor Specificity of the H3 Hemagglutinin Based on Species of Origin. *Virology* **1983**, *127*, 361–373.
14. Zhang, W.; Shi, Y.; Qi, J.; Gao, F.; Li, Q.; Fan, Z.; Yan, J.; Gao, G. F. Molecular Basis of the Receptor Binding Specificity Switch of the Hemagglutinins from Both the 1918 and 2009 Pandemic Influenza A Viruses by a D225G Substitution. *J. Virol.* **2013**, *87*, 5949–5958.
15. Shi, Y.; Zhang, W.; Wang, F.; Qi, J.; Wu, Y.; Song, H.; Gao, F.; Bi, Y.; Zhang, Y.; Fan, Z.; et al. Structures and Receptor Binding of Hemagglutinins from Human-Infecting H7N9 Influenza Viruses. *Science* **2013**, *342*, 243–247.
16. Xiong, X.; Coombs, P. J.; Martin, S. R.; Liu, J.; Xiao, H.; McCauley, J. W.; Locher, K.; Walker, P. A.; Collins, P. J.; Kawaoka, Y.; et al. Receptor Binding by a Ferret-Transmissible H5 Avian Influenza Virus. *Nature* **2013**, *497*, 392–396.
17. Quinten, M.; Kreibig, U.; Schönauer, D.; Genzel, L. Optical Absorption Spectra of Pairs of Small Metal Particles. *Surf. Sci.* **1985**, *156*, 741–750.
18. Leuvering, J. H. W.; Thal, P. J. H. M.; Waart, M. v. d.; Schuurs, A. H. W. M. Sol Particle Agglutination Immunoassay for Human Chorionic Gonadotrophin. *Fresenius' Z. Anal. Chem.* **1980**, *301*, 132–132.
19. Elghanian, R.; Storhoff, J. J.; Mucic, R. C.; Letsinger, R. L.; Mirkin, C. A. Selective Colorimetric Detection of Polynucleotides Based on the Distance-Dependent Optical Properties of Gold Nanoparticles. *Science* **1997**, *277*, 1078–1081.
20. Zagorovsky, K.; Chan, W. C. A Plasmonic DNAzyme Strategy for Point-of-Care Genetic Detection of Infectious Pathogens. *Angew. Chem., Int. Ed.* **2013**, *52*, 3168–3171.
21. Rosi, N. L.; Mirkin, C. A. Nanostructures in Biodiagnostics. *Chem. Rev.* **2005**, *105*, 1547–1562.
22. Boisselier, E.; Astruc, D. Gold Nanoparticles in Nanomedicine: Preparations, Imaging, Diagnostics, Therapies and Toxicity. *Chem. Soc. Rev.* **2009**, *38*, 1759–1782.
23. Marradi, M.; Chioldo, F.; García, I.; Penadés, S. Glyconanoparticles as Multifunctional and Multimodal Carbohydrate Systems. *Chem. Soc. Rev.* **2013**, *42*, 4728–4745.
24. Driskell, J. D.; Jones, C. A.; Tompkins, S. M.; Tripp, R. A. One-Step Assay for Detecting Influenza Virus Using Dynamic Light Scattering and Gold Nanoparticles. *Analyst* **2011**, *136*, 3083–3090.
25. Marín, M. J.; Rashid, A.; Rejzek, M.; Fairhurst, S. A.; Wharton, S. A.; Martin, S. R.; McCauley, J. W.; Wileman, T.; Field, R. A.; Russell, D. A. Glyconanoparticles for the Plasmonic Detection and Discrimination between Human and Avian Influenza Virus. *Org. Biomol. Chem.* **2013**, *11*, 7101–7107.
26. Lee, C.; Gaston, M. A.; Weiss, A. A.; Zhang, P. Colorimetric Viral Detection Based on Sialic Acid Stabilized Gold Nanoparticles. *Biosens. Bioelectron.* **2013**, *42*, 236–241.
27. Collins, B. E.; Paulson, J. C. Cell Surface Biology Mediated by Low Affinity Multivalent Protein–Glycan Interactions. *Curr. Opin. Chem. Biol.* **2004**, *8*, 617–625.
28. Blixt, O.; Head, S.; Mondala, T.; Scanlan, C.; Huflejt, M. E.; Alvarez, R.; Bryan, M. C.; Fazio, F.; Calarese, D.; Stevens, J.; et al. Printed Covalent Glycan Array for Ligand Profiling of Diverse Glycan Binding Proteins. *Proc. Natl. Acad. Sci. U.S.A.* **2004**, *101*, 17033–17038.
29. Zhou, Y.; Wang, S.; Zhang, K.; Jiang, X. Visual Detection of Copper(II) by Azide- and Alkyne-Functionalized Gold Nanoparticles Using Click Chemistry. *Angew. Chem., Int. Ed.* **2008**, *47*, 7454–7456.
30. Love, J. C.; Estroff, L. A.; Kriebel, J. K.; Nuzzo, R. G.; Whitesides, G. M. Self-Assembled Monolayers of Thiolates on Metals as a Form of Nanotechnology. *Chem. Rev.* **2005**, *105*, 1103–1169.
31. Watanabe, T.; Kiso, M.; Fukuyama, S.; Nakajima, N.; Imai, M.; Yamada, S.; Murakami, S.; Yamayoshi, S.; Iwatsuki-Horimoto, K.; Sakoda, Y.; et al. Characterization of H7N9 Influenza A Viruses Isolated from Humans. *Nature* **2013**, *501*, 551–555.

32. Belser, J. A.; Gustin, K. M.; Pearce, M. B.; Maines, T. R.; Zeng, H.; Pappas, C.; Sun, X.; Carney, P. J.; Villanueva, J. M.; Stevens, J.; *et al.* Pathogenesis and Transmission of Avian Influenza A (H7N9) Virus in Ferrets and Mice. *Nature* **2013**, *501*, 556–559.
33. Zhang, Q.; Shi, J.; Deng, G.; Guo, J.; Zeng, X.; He, X.; Kong, H.; Gu, C.; Li, X.; Liu, J.; *et al.* H7N9 Influenza Viruses Are Transmissible in Ferrets by Respiratory Droplet. *Science* **2013**, *341*, 410–414.
34. Xiong, X.; Martin, S. R.; Haire, L. F.; Wharton, S. A.; Daniels, R. S.; Bennett, M. S.; McCauley, J. W.; Collins, P. J.; Walker, P. A.; Skehel, J. J.; *et al.* Receptor Binding by an H7N9 Influenza Virus from Humans. *Nature* **2013**, *499*, 496–499.
35. Liao, H. Y.; Hsu, C. H.; Wang, S. C.; Liang, C. H.; Yen, H. Y.; Su, C. Y.; Chen, C. H.; Jan, J. T.; Ren, C. T.; Chen, C. H.; *et al.* Differential Receptor Binding Affinities of Influenza Hemagglutinins on Glycan Arrays. *J. Am. Chem. Soc.* **2010**, *132*, 14849–14856.
36. Tharakaraman, K.; Jayaraman, A.; Raman, R.; Viswanathan, K.; Stebbins, N. W.; Johnson, D.; Shriner, Z.; Sasisekharan, V.; Sasisekharan, R. Glycan Receptor Binding of the Influenza A Virus H7N9 Hemagglutinin. *Cell* **2013**, *153*, 1486–1493.
37. Guo, C. T.; Takahashi, N.; Yagi, H.; Kato, K.; Takahashi, T.; Yi, S. Q.; Chen, Y.; Ito, T.; Otsuki, K.; Kida, H.; *et al.* The Quail and Chicken Intestine Have Sialyl-Galactose Sugar Chains Responsible for the Binding of Influenza A Viruses to Human Type Receptors. *Glycobiology* **2007**, *17*, 713–724.
38. Hirst, G. K. The Quantitative Determination of Influenza Virus and Antibodies by Means of Red Cell Agglutination. *J. Exp. Med.* **1942**, *75*, 49–64.
39. Frens, G. Controlled Nucleation for the Regulation of the Particle Size in Monodisperse Gold Suspensions. *Nat. Phys. Sci.* **1973**, *241*, 20–22.
40. Ghosh, S. K.; Pal, T. Interparticle Coupling Effect on the Surface Plasmon Resonance of Gold Nanoparticles: From Theory to Applications. *Chem. Rev.* **2007**, *107*, 4797–4862.